

Enhancing the Development Rate Model For Optimum Simulation Capability in the Sub-Half-Micron Regime.

Graham Arthur, Brian Martin,⁺ Chris A. Mack.*

Central Microstructure Facility, Rutherford Appleton Laboratory, Chilton, Didcot, Oxon.
OX11 0QX, UK.

⁺ GEC Plessey Semiconductors, Tamerton Road, Roborough, Plymouth, Devon. PL6 7BQ, UK.

* FINLE Technologies Inc., P.O. Box 162712, Austin TX, 78716, USA.

ABSTRACT.

Methods used in the extraction of lithographic modelling parameters for simulation packages such as PROLITH/2¹ are examined. The results reveal hitherto unconsidered aspects of the development process which, when implemented in the simulations, give improved agreement with practical results with regard to characteristics such as resolution, depth-of-focus, linearity and dense/isolated bias.

These refinements, which are particularly influential in the sub-half-micron regime, include the variation in photoresist dissolution properties as a function of depth into the resist film and also a small but powerful development "notch" which is observed in the development rate vs. PAC concentration curve as it approaches the minimum dissolution rate.

This work therefore shows that current development models may not be adequate for some applications, and that great care must be taken in deriving and using the correct set of parameters for any one situation.

Keywords: Optical lithography, Simulation, Parameter extraction, Development rate monitor, PROLITH/2.

1. INTRODUCTION.

Advanced IC manufacture will soon require dimensions below 200nm to be routinely obtained and it is generally accepted that optical lithography will remain a key tool in the industry. Therefore, the demand for optical resolution at, or below, the wavelength of the imaging system is increasing. As an example, 0.35 micron lithography using i-line (365nm) wavelength radiation is already being offered by stepper and resist manufacturers and is being introduced into production, whilst 0.24 micron dimensions have been demonstrated in research laboratories at the same wavelength. These improvements in optical lithography have been brought about by investment in lens technology and manufacture together with a range of enhancement techniques, including phase-shifting masks (PSM) and off-axis illumination. In addition, resist vendors are now supplying highly specialised photoresists; for example, some are intended for use with PSMs while others are claimed to be critical layer specific.

One of the consequences of setting up a new process, using advanced steppers and resists with a wider range of variables, is that IC manufacturers increasingly rely on computer simulation programs such as PROLITH/2 to support process optimisation. However, the resist and development input parameters^{2,3} for such simulations are not always readily obtainable and may be of unknown accuracy (the techniques for measurement and parameter extraction do not have recognised standard methods).

Development rate vs. PAC concentration, $R(m)$, curves lie at the heart of all such simulations and, in addition to accurate derivation, any loss of detailed information arising from their conversion to sets of development parameters can affect the simulation results and this is particularly noticeable in the sub-half-micron regime.

This paper will examine development rate monitor (DRM) data and the derived R(m) curves in detail, highlighting variations in the curves which are not predicted by the conventional development parameters. Modifications to the R(m) curves to incorporate these variations using the development rate file option available in PROLITH/2 have been carried out and a noticeable improvement in the simulated results have been observed, not only in the overall profile shape, but also in terms of characteristics such as resolution, depth-of-focus and dense/isolated bias. Practical results obtained on a high performance commercial wafer stepper and SEM photographs are used throughout to fully support the simulation work and the parameters derived.

2. BACKGROUND.

2.1. Resist characterisation.

Conventional, positive-acting photoresists such as those typified by most commercially available diazonaphthoquinone (DNQ)-based photoresists are normally composed of a base resin and photoactive compound (PAC). Some resists also contain a dye, increasing the opacity of the base resin in order to reduce swing curve and notching effects. However the dye is not photosensitive and is simply considered as part of the base resin.

The behaviour of the resist which has been fully described elsewhere^{2,4} can be divided into two phases: exposure, described by the parameters A, B, C and development, which has been described by a number of different models, with the most popular being those originally devised for use in PROLITH/2.

The exposure parameters A, B and C are relatively easily determined by measuring the transmitted intensity of a uniform beam of light, at the exposure wavelength, through a resist film of known thickness on a transparent substrate. A typical result is shown graphically in Figure 1.

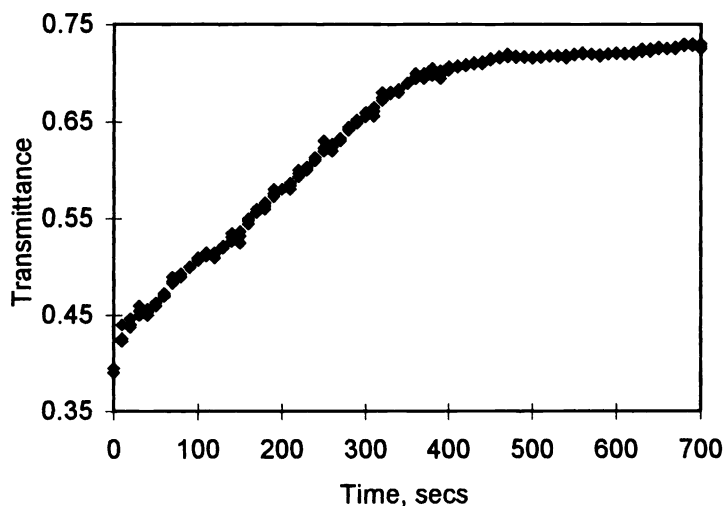


Figure 1. Typical transmittance vs. time curve for the derivation of ABC parameters.

The exposure parameters A, B and C are defined thus:

$$A = \left(\frac{1}{d} \right) \ln \left[\frac{T(\infty)}{T(0)} \right]$$

$$B = - \left(\frac{1}{d} \right) \ln T(\infty)$$

$$C = \frac{A + B}{AI_0T(0) [1 - T(0)]} \frac{dT(0)}{dt}$$

where: d = resist thickness
 $T(0)$ = transmittance at time = 0 (unexposed resist)
 $T(\infty)$ = transmittance at time = ∞ (fully exposed resist)
 I_0 = intensity of incident radiation

Therefore it can be seen that A describes the degree of change in the transmittance of the resist following complete exposure and variation of the initial concentration of PAC will change only this parameter. B is a measure of the intrinsic absorption of the base resin of the resist after complete exposure (assuming the reaction products of the exposure process do not contribute to resist absorption). Addition or subtraction of an absorbing dye will alter only this value. Finally, C describes the bleaching speed. For exposure intensity, I and time, t, the mathematical relationship between the normalised PAC concentration, m and depth into resist, z is given by:

$$\frac{\partial I(z, t)}{\partial z} = -I(z, t)[Am(z, t) + B]$$

$$\frac{\partial m(z, t)}{\partial T} = -I(z, t)m(z, t)C$$

During development two competing processes take place. One of these inhibits the photoresist dissolution rate, whilst the other enhances this rate.

A film composed entirely of the base resin is moderately soluble in an aqueous alkaline developer. However, when the PAC is present solubility is reduced. Hence the term "inhibitor" is used to describe the role of the PAC which typically constitutes 30% of the resist, the remaining 70% being the base resin. The photochemical action of the incident radiation bleaches (destroys) the PAC, restoring the solubility of the resist. More significantly, during exposure, carboxylic acid is created as one of the reaction products and this greatly enhances the solubility of the resin. The combination of these reactions therefore creates a difference in the dissolution rate between the exposed and unexposed areas in the ratio of approximately 20,000:1 and thus enables resist to be used in its intended role in image transfer.

The "Original Mack" model describing the development process has parameters R_{\max} , R_{\min} , m_{th} and n. Here R_{\max} and R_{\min} are respectively the maximum and minimum development rates whilst m_{th} , the PAC concentration threshold value is located at the point of inflection in the R(m) curve. The developer selectivity value, n is related to resist contrast and the slope of the curve through m_{th} . These parameters are used to describe the development rate, R as a function of the normalised PAC concentration, m, thus:

$$R = R_{\max} \frac{(a - 1)(1 - m)^n}{a + (1 - m)^n} + R_{\min}$$

where: $a = \frac{(n + 1)}{(n - 1)} (1 - m_{th})^n$

The development model given above was derived from a kinetic model based purely on the enhancement of the dissolution rate. A later "Enhanced Mack" model was developed² and considered both the inhibition and the enhancement effects. This model is a superset of the original model and R(m) is now described by:

$$R = R_{\text{resin}} \frac{1 + k_{\text{enh}}(1 - m)^n}{1 + k_{\text{inh}}(m)^l}$$

and $R_{\text{max}} = R_{\text{resin}}(1 + k_{\text{enh}})$

$$R_{\text{min}} = \frac{R_{\text{resin}}}{1 + k_{\text{inh}}}$$

where: R_{resin} = resin development rate
 l = inhibition selectivity
 k_{enh} = constant representing the enhancement mechanism
 k_{inh} = constant representing the inhibition mechanism

2.2. Parameter extraction.

Whichever model is selected, an $R(m)$ curve must be derived from practical experiments before curve-fitting can be performed and the parameters extracted. This can be achieved by carrying out a large number of exposures and developments by hand^{6,7} (the so-called Poor Man's DRM) or by the preferred method of using one of the now commercially available DRMs which are capable of revealing subtle information not seen with the former method.

The DRM data can be output in many formats but the one used here is that of development rate vs. depth into resist. An example of this is shown in Figure 2. In this example a reduction in development rate arising from surface inhibition can be seen to extend from the top surface to an approximate depth of 80nm whilst the bulk development rates continue from there to approximately 800nm depth. Also visible in the majority of the curve are residual standing waves which have not been fully removed and these can be used to estimate the PAC diffusion length during post exposure bake (PEB). Great care is required in measuring the surface inhibition as the uppermost residual standing wave can cause the degree of inhibition to be overestimated. Less obvious at this time is the substrate inhibition, but this will become more evident after further processing.

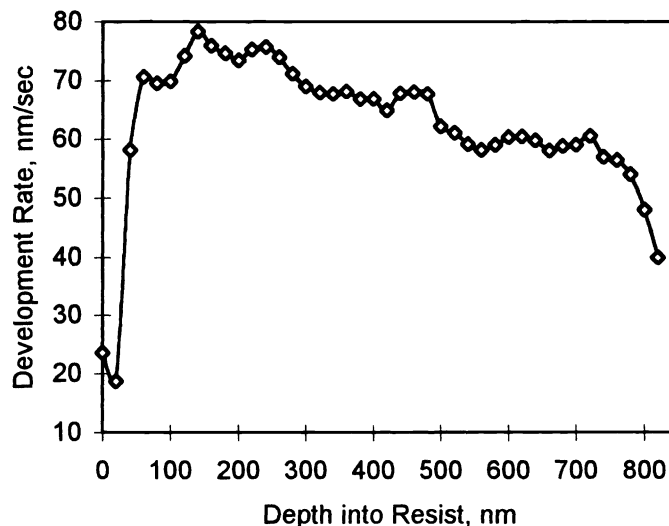


Figure 2. A typical example of data from a DRM as a plot of development rate vs. depth into resist. The top of the resist is at $z=0$ nm and full film thickness is 820nm. The effects due to surface inhibition can be seen from $z=0$ to ~ 80 nm and residual standing waves are evident over the majority of the curve.

The DRM curves can thus be used to give the development rate as a function of depth into resist film, $R(z)$. Knowledge of the exposure dose, optical parameters (n , k) of the substrate and the Dill A, B, C parameters of the resist, when used with the theory outlined earlier can be used to establish the PAC concentration as a function of depth, $m(z)$. Combining these

results arrives at the required $R(m)$ curve. Previously, the $R(m)$ data would now be fitted to the chosen development model thus extracting the parameter set. Ideally, the $R(m)$ data used for this curve-fitting procedure should not include data which is close (typically 100nm) from either the top or bottom of the resist film as these regions are not likely to be fully representative of the bulk dissolution characteristics due to possible inhibition effects. An example of such a fit is shown in Figure 3(a).

It should be remembered that the final values of $m(z)$, calculated above, must also include the PAC re-distribution resulting from the diffusion which takes place during the PEB and as already mentioned this can be used to estimate the diffusion length. If a single DRM trace, similar to that shown in Figure 2, is considered, the resulting $R(m)$ curve should be smooth. If an incorrect value for the diffusion length is selected, there will be an oscillation in the $R(m)$ curve along one of the axes depending upon whether the diffusion length selected was too high or too low (e.g. an oscillation parallel to the m -axis is seen if too low a diffusion length is used). In practice zero oscillation is rare and a minimum level would be sought.

Accurate simulation is largely dependant upon that part of the $R(m)$ curve where, in the example given, $R < 25 \text{ nm/sec}$ and in order to improve the curve-fit, some experimenters have used the logarithm of the development rate during the curve-fitting process to place increased emphasis on that part of the curve. Indeed, this improves the fit in this region as shown in Figure 3(b), but if the development axis is restored to a linear scale (Figure 3(c)), the remainder of the curve is often well removed from the practical data and this cannot be said to be a true characterisation of the resist. This method of curve-fitting is often revealed by an excessively high value of n (using the Original Mack model). Realistic values typically lie in the range 1-3 for an older resist, 3-7 for a typical resist and up to approximately 10 for a high performance, state-of-the-art resist, whereas higher values ($n=35$ has been quoted) must be considered highly suspect for a conventional DNQ-based novolac photoresist.

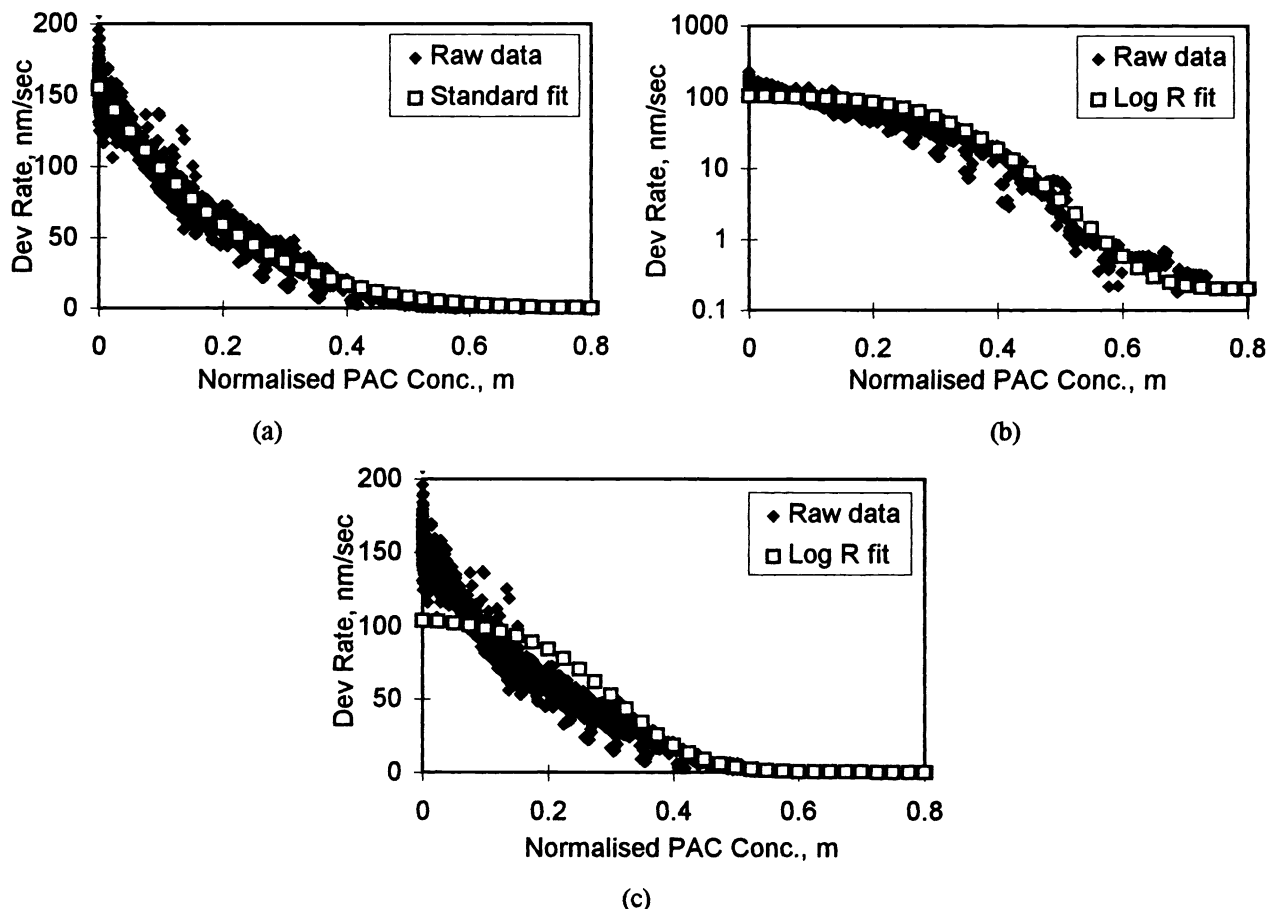


Figure 3. Typical example of an $R(m)$ curve showing the DRM data and the 2 fitting techniques described. (a) Standard fit, (b) Using Log R to enhance the fit at low development rates, (c) Graph (b) with the development rate restored to a linear scale and showing the deviation of the fitted curve to practical data at low PAC concentrations. However, when compared to (a), the improved fit at $m > 0.45$ is evident.

2.3. Additional extractable characteristics.

If Figure 3(a) is examined in detail for $0.4 < m < 0.6$ (see Figure 4), further information may be gleaned. Firstly, as R approaches R_{\min} , the development rate of the practical data drops rapidly and deviates from the fitted curve, producing a development “notch.” Although small, this notch is a powerful aspect of the $R(m)$ curve and its effect will be seen later. Secondly, the individual curves are seen to turn back on themselves as the development approaches the substrate. This reduction in the PAC concentration is due to reflection of the exposing radiation at the substrate. However a corresponding increase in the development rate, which might be expected, is not seen. The reduced development rate at this location in the resist film, can be attributed to substrate inhibition and extends for a typical thickness of 50-100nm above the substrate.

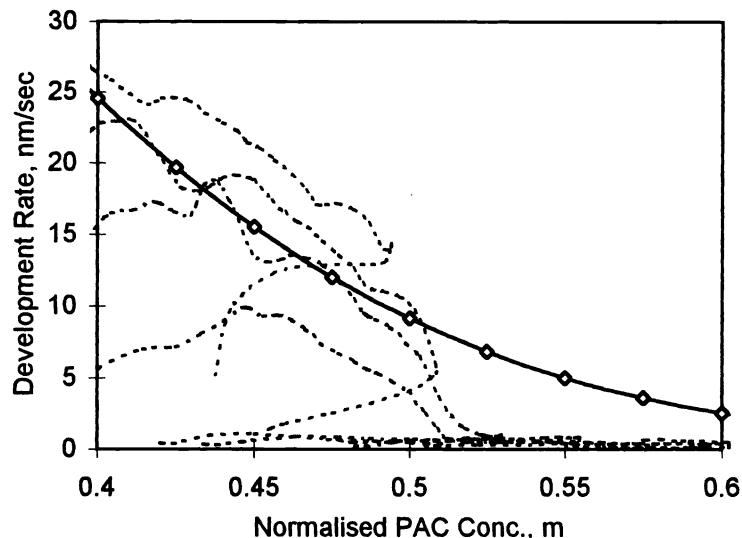


Figure 4. A close-up of $R(m)$ data for $0.4 < m < 0.6$, showing reversal of the individual curves arising from the substrate inhibition. Also seen is the rapid reduction in development rate compared with that predicted by the fitted curve. The $R(m)$ data from DRM measurements is shown as dotted lines and the fit obtained using the full range of data (i.e. from $m=0$ to 1) and the “Original Mack” development model is shown as the solid line with symbols.

Finally, returning to the full $R(m)$ curves, if the DRM data is divided into sub-layers within the resist film (in this case 4 layers each 25% of the total film thickness), they can be plotted individually to reveal the development characteristics of the resist as a function of depth, $R(m,z)$. The surface and substrate inhibited layers may also be processed separately (slightly reducing the thicknesses of the top and bottom sub-layers) to give further information. An example of this procedure is given in Figures 5-8.

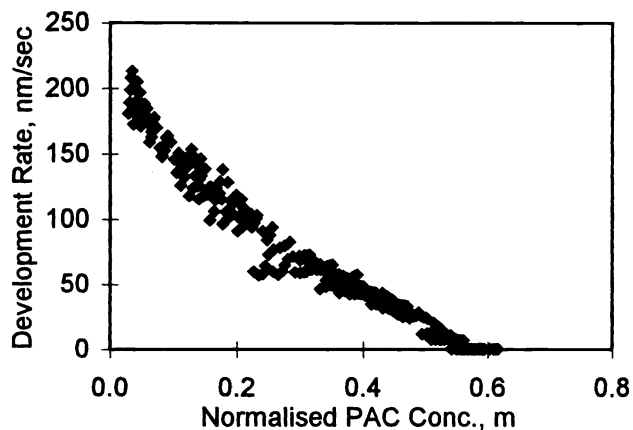


Figure 5. Typical $R(m)$ data for $z = 0-25\%$.

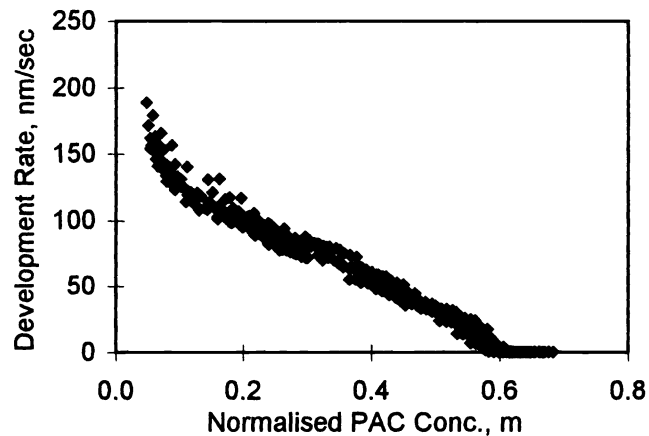


Figure 6. Typical $R(m)$ for $z = 26-50\%$.

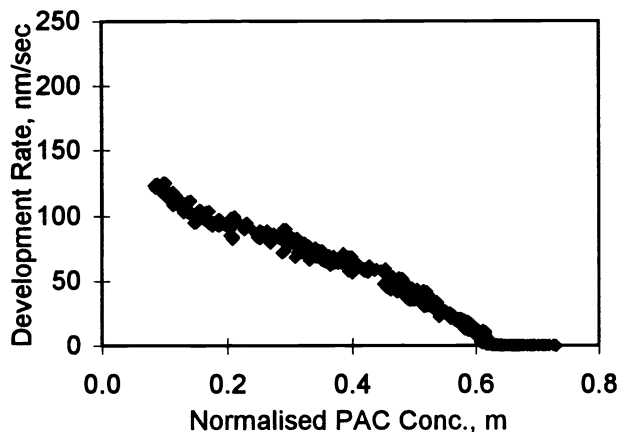


Figure 7. Typical R(m) data for $z = 51-75\%$.

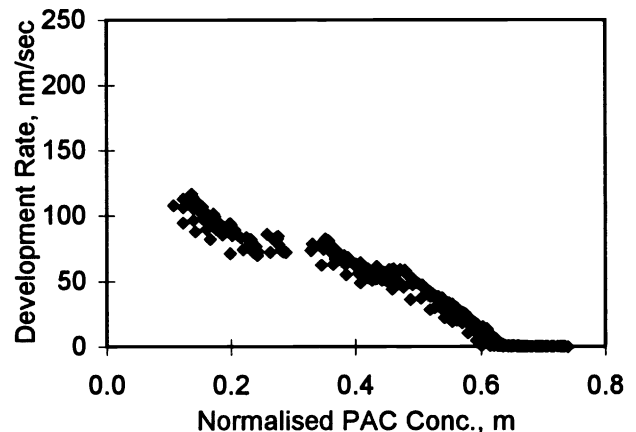


Figure 8. Typical R(m) data for $z = 76-100\%$.

3. EXPERIMENTAL.

The work presented here examined 8 photoresists from 2 vendors. 2 types of DRM were used: a Perkin-Elmer machine and the more recent and refined RDA-790 instrument from Litho Tech Japan which is better able to resolve both surface and substrate inhibitions as well as the residual standing waves.

Bare silicon substrates were used throughout and film thicknesses in all cases were set at a minimum energy in-coupling point on the swing curve giving values of 0.86, 0.975 or 1.07 microns. Exposures were varied from $0\text{mJ}/\text{cm}^2$ to $520\text{mJ}/\text{cm}^2$ in small increments and then in larger increments up to a maximum of $3000\text{mJ}/\text{cm}^2$. Softbake (SB) and PEB were as per the vendors recommended standard process conditions (SB= 90°C , PEB= 110°C , both for 60 seconds). Up to 36 exposure levels were measured for each resist. SEM images of dense and isolated lines at various degrees of defocus were also printed, using the exposure-to-size found at best focus, under the same process conditions. In one case, a resist specifically designed for use on a bottom anti-reflective coating (ARC), images were printed onto a 110nm layer of ARC. On-axis and off-axis illumination exposures were available. Focus-exposure (F-E) plots of some of the resists were also measured to allow a more rigorous comparison. The Dill exposure parameters, A, B, C, were provided by the resist vendors. R(m,z) data was extracted as outlined above:

1. R(z) was calculated from the DRM data for each exposure run.
2. m(z) was calculated using PROLITH/2 v5.06 and assumed a typical value of PEB diffusion length. The required data is found within PROLITH/2 in the output file, Sr_peg.dat.
3. R(m) was calculated and plotted from (1) and (2).
4. (1), (2) and (3) were repeated for different values of diffusion length until an optimum value was obtained.
5. R(m) curves were divided into sub-layers as described earlier.
6. Each sub-layer was curve-fitted to either the Original or Enhanced Mack model. The model giving the overall best fit being the one finally selected.
7. Using the modelling parameters derived in (6), an R(m) table for each sub-layer was generated using increments in m of 0.025.
8. The R(m) tables were edited by hand to accurately follow the development "notch," if present.
9. The individual R(m) tables were assembled to form R(m,z) development rate files suitable for use in PROLITH/2.
10. Simulation was compared with the SEM images and F-E plots to verify the development rate file data.

In addition to the procedure described above a "standard" parameter extraction was performed to allow a direct comparison between the R(m,z) development rate files and conventionally derived sets of modelling parameters.

4. RESULTS.

A wide range of variations was observed in the behaviour of the $R(m,z)$ curves for the various photoresists. Unfortunately space does not permit inclusion of all graphs but a selection of the results is given in Figures 9(a-c) which show the results for 3 of the resists. Resist 9(a) shows no obvious surface inhibition, but does exhibit substrate inhibition, whilst the resist in Figure 9(b) shows both surface and substrate inhibition. Figure 9(c) also shows surface and substrate inhibition, but these are omitted for clarity. This particular resist does however, demonstrate the considerable difference between the sub-layers. Following examination of results for all 8 photoresists, the following overall observations were made:

1. The diffusion lengths were found to be $50\text{nm} \pm 2.5\text{nm}$. The DRM data obtained via the Perkin-Elmer instrument could not be used as the resolution was too low to reliably identify the standing waves. In these cases, a generic value of 50nm was assumed.
2. Ignoring the surface inhibition region, R_{max} is greatest in the top 25% and decreases as depth into resist increases. This is clearly demonstrated in Figure 9(c).
3. At normal exposure levels, where m is unlikely to be below 0.15, the photospeed of the resist increases as depth increases. In particular, for $0.3 < m < 0.7$ it is seen that, for the same PAC concentration, the development rates are generally higher as depth increases. Clearly this means that the curves must cross somewhere between $m=0$ and $m=0.3$. Both these points are visible in Figures 9(a-c).
4. The greatest change between curves occurs between the top 2 sub-layers, whereas the bottom 2 sub-layers are very similar. At this time, the reason for this is not known and several explanations have been given. One such is solvent content and this is tentatively supported by, for example, Figure 7 in reference 8 where the solvent content rises with depth into resist in a similar manner.
5. All resists exhibit substrate inhibition.
6. Only 1 resist does not show any obvious surface inhibition.
7. Although less obvious in some, the development "notch" is present in all resists.
8. The location of the development "notch" tends to move to higher values of m as depth increases.

In addition to these observations, the following 2 points are made, but cannot be confirmed without further experimentation:

8. Thicker resist films tend to exhibit the greatest change in characteristics between sub-layers. Again this may support the proposition that solvent content is responsible for the observed effects as a thicker resist film is likely to retain a greater quantity of solvent under the same process conditions.
9. The older resists show the smallest development "notches" whereas the newer, higher performance resists show larger "notches." This may be a consequence of the addition of "speed enhancers" or a blend of more than 1 novolac in their composition.

Comparison with practical results are shown in Figures 10 and 11. Figure 10 includes a through-focus plot for 0.3 micron dense lines and various points are picked out where SEM, $R(m,z)$ and conventional parameter images are shown. Figure 11 shows practical and simulated F-E plots for another of the resists again with $R(m,z)$ and conventional parameter simulations for comparison. The actual lens aberrations were not available, but a typical set was input via the Typical.zrn file, as supplied with PROLITH/2. 3% flare was also included.

It is clear from Figures 10 and 11, that the $R(m,z)$ development rate files give superior results compared with the standard parameter sets. In addition, the dense-isolated bias was calculated. For example, for the resist in Figure 10, the $R(m,z)$ file gave excellent correlation with the practical measurements whereas, the conventionally derived parameter set gave a bias of the opposite sign (i.e. the isolated line was narrower when it should have been wider). This can be wholly attributed to the development "notch" as the remainder of the $R(m)$ curves are very similar.

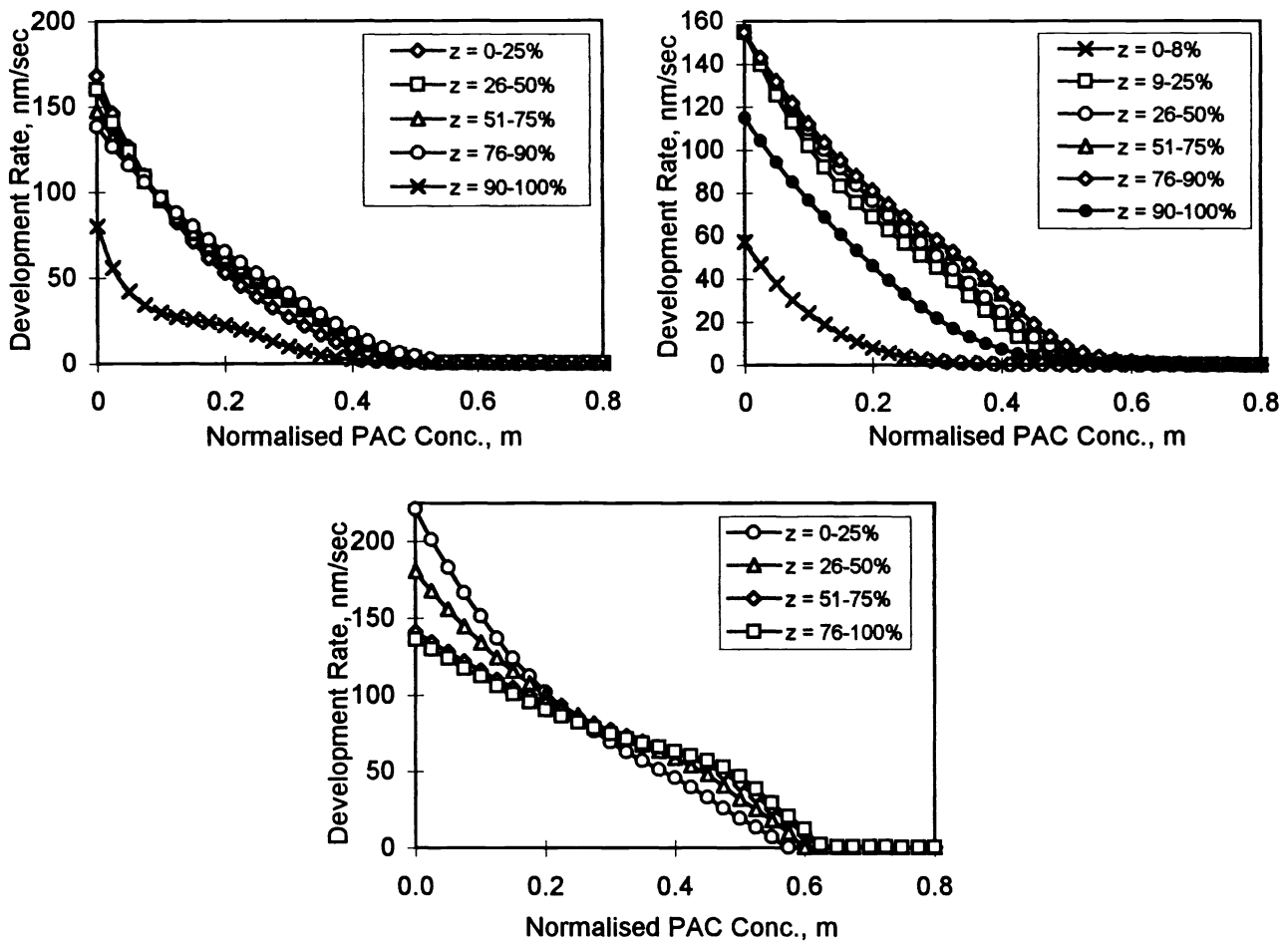


Figure 9. $R(m,z)$ curves for 3 of the photoresists examined.

Although a subjective test, the overall appearance of the profiles produced using the $R(m,z)$ development rate files were seen to be in better agreement with the SEM images. The $R(m,z)$ rate file-generated profiles in Figure 10 have steeper wall angles (due to the increasing photospeed in the lower levels of the resist layer opening out those parts of the exposed regions) and the flat, well defined top surface of the profiles are replicated to a better degree of accuracy. Indeed, some tests with and without the inclusion of a surface inhibition layer showed very little difference. In particular, notice that the corner between the sidewall and the top shows a sharp angle rather than a more rounded transition. This suggests that the development “notch” is largely responsible for this part of the profile rather than the surface inhibition, as has previously been believed. The major contribution of the surface inhibition appears to be a reduction in the resist loss at the top of the profile. However, this is difficult to confirm practically as the difference is only $\sim 20\text{nm}$ and pre-exposure SEMs are not available. To test this further, some simulations were carried out using the conventional development parameter sets, altering the surface inhibition values by trial and error in an attempt to replicate the practical profiles. In most cases this was not achieved to the level seen using the $R(m,z)$ files, even when highly exaggerated values of surface inhibition were input. Therefore, this part of the profile is attributed mainly to the development “notch” and appears to be created as the development effectively “switches off” very rapidly as the “notch” is reached. This is further confirmed by viewing the post-PEB PAC distribution contours using PROLITH/2 where the final sidewall contour closely follows the m value found at the bottom of the development “notch.” These effects show that the changing photospeed and the “notch” give the resist a higher contrast than would be predicted by the $R(m)$ curve derived by the conventionally extracted parameter set.

Finally, 0.24 micron dense lines, using off-axis (annular) illumination, were compared with simulation. Figure 12 shows that the conventional parameter set was not able to achieve full-depth profiles whereas the $R(m, z)$ file was able to accurately replicate the practical results.

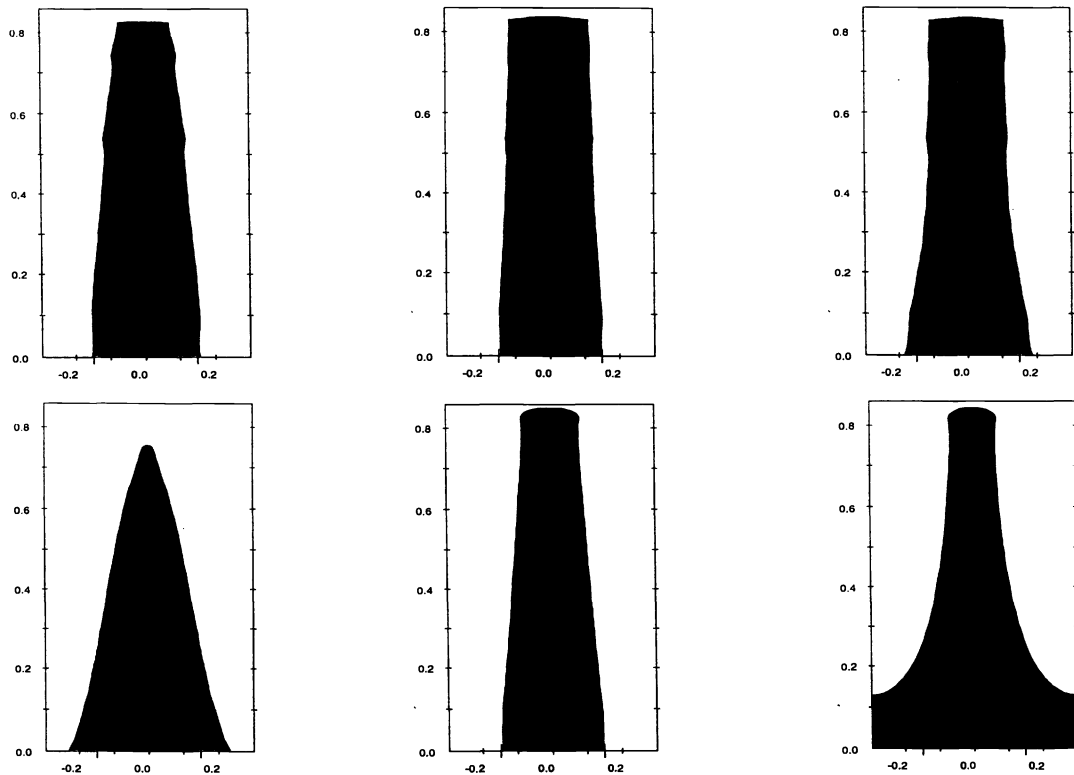
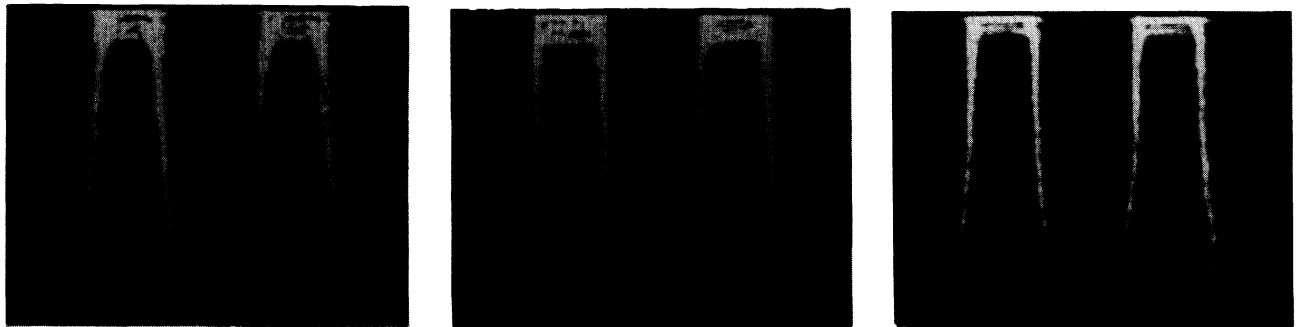
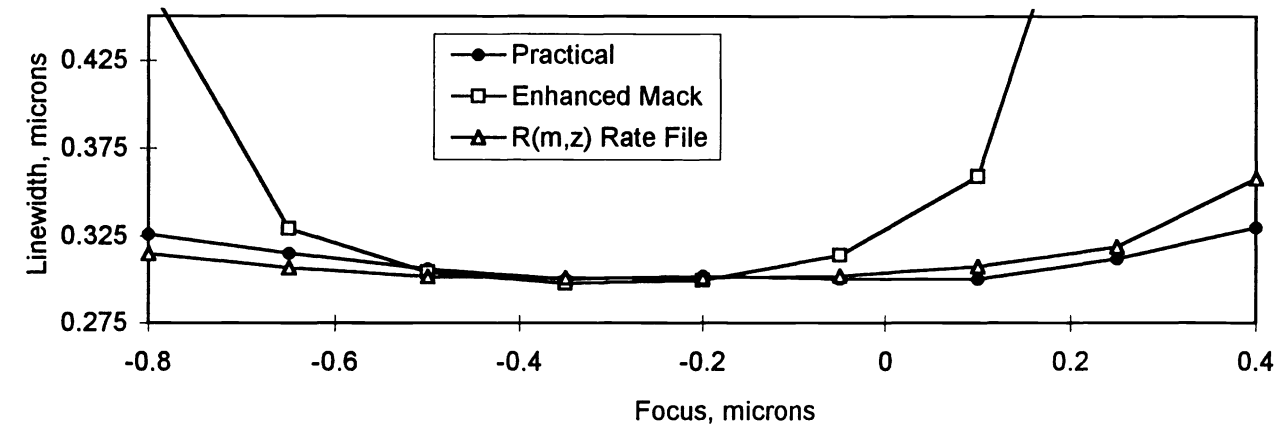


Figure 10. Comparison of practical data with simulation results using an R(m,z) development rate data file and those from a conventionally derived parameter set, for the resist in Figure 9(b). From top to bottom are: through-focus CD measurements, SEM images, profiles from the R(m,z) data file and the conventionally derived parameter set results. From left to right, the focus settings for the profiles are: -0.8 microns, best focus (-0.3 microns) and 0.4 microns.

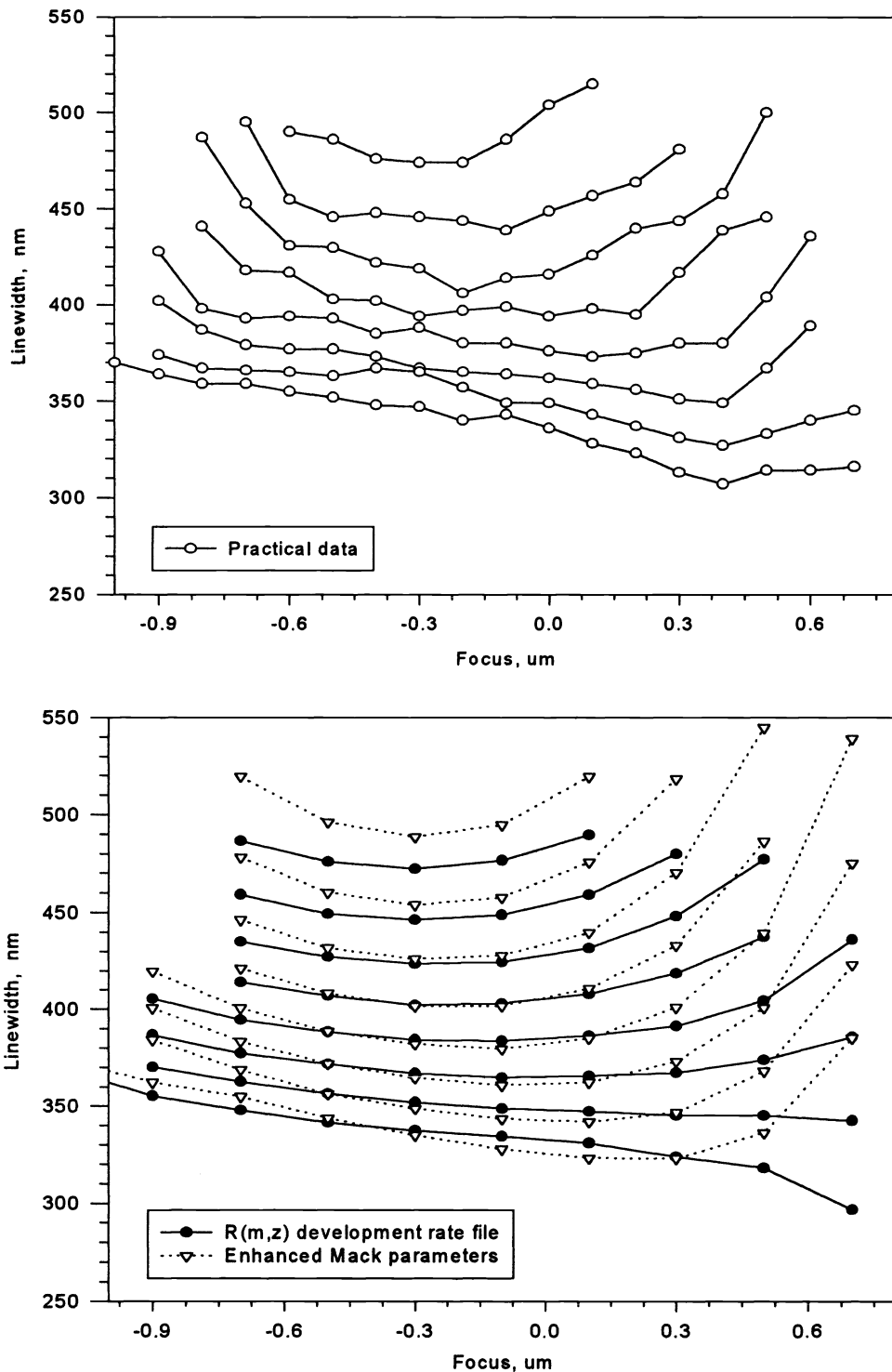


Figure 11. A comparison between F-E plots from practical data, the $R(m,z)$ development rate file and the standard parameter set. Exposures are from $280\text{-}350\text{mJ/cm}^2$. The $R(m,z)$ simulation shows improved accuracy for the higher exposures at large positive defocus values whilst that from the parameter set has reduced exposure latitude compared to the practical data, indicated by the increased vertical spread of the curves. Although not shown here, simulated resist profiles using the parameter set also show reduced wall angle and greater resist loss.

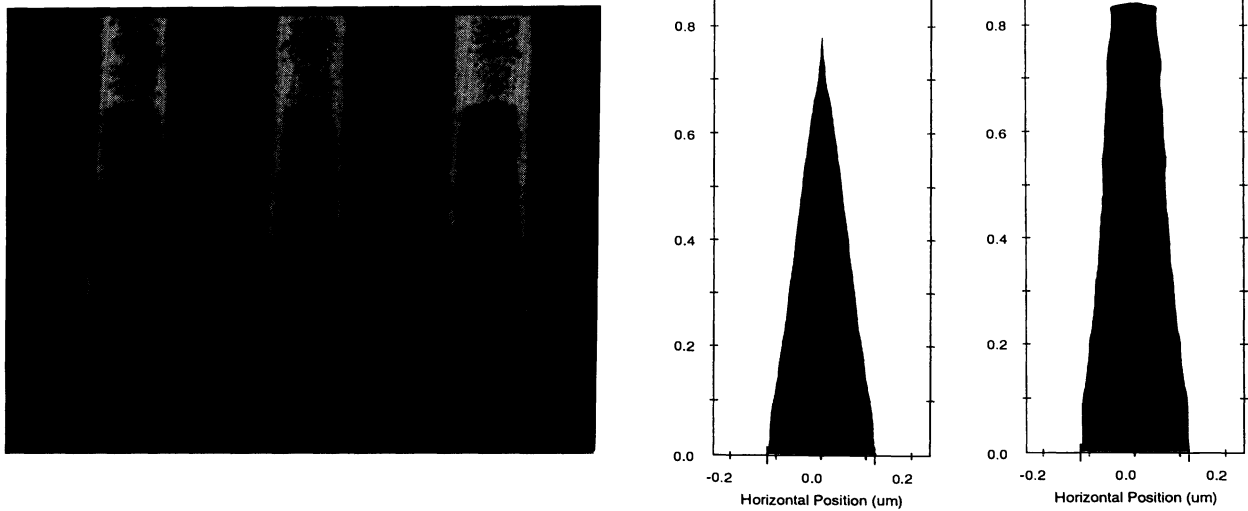


Figure 12. A comparison between 0.24 micron dense lines using off-axis (annular) illumination. The middle image is the best obtained by the conventional parameter set, whereas that produced using the R(m,z) file is shown to the right

5. CONCLUSIONS.

The work presented here, has successfully shown an improvement in the simulation of sub-half-micron resist images compared with those obtained using a conventionally derived set of development parameters. Indeed, some situations are successfully simulated when the parameter set predicts that imaging is not possible.

The drawback to the proposed development rate file usage is that it is specific to a particular resist film thickness and cannot be transferred to a new film thickness with confidence. However, this must be equally true when using a standard set of development parameters. Investigations into the cause of the R(z) behaviour and the development "notch" are on-going, as well as new models to account for them.

6. ACKNOWLEDGEMENTS.

The authors would like to acknowledge the help of JSR Electronics N.V., JSR Japan, Hoechst AG and Hoechst Celanese Corporation for providing DRM data and SEM images, in particular Makoto Murata and Brian Hickmott of JSR and Ralph Dammel and Neville Eilbeck of Hoechst. The support of the SHAPE project is also acknowledged.

7. REFERENCES.

1. PROLITH/2, FINLE Technologies, Inc., P.O. Box 162712, Austin, Texas 78716, USA.
2. Dill, F.H., et al., "Characterization of Positive Photoresist." *IEEE Transactions on Electron Devices*, Vol. ED-22, No.7, July 1975, pp 445-452.
3. Mack, C.A., "A Comprehensive Optical Lithography Model," *Optical Microlithography IV*, Vol. 538, SPIE, 1985, pp207-220.
4. Dammel, R., *Diazonaphthoquinone-Based Resists*, SPIE Optical Engineering Press, 1993.
5. Mack, C.A., "A New Kinetic Model to Describe Photoresist Development," *Journal of the Electrochemical Society*, Vol. 139, No. 4, April 1992, pp L35-L37.
6. Thornton, S.H., Mack, C.A., "Lithography Model Tuning: Matching Simulation to Experiment," *Optical Microlithography IX*, Vol. 2716, SPIE, 1996, pp223-235.
7. Fahey, K.P., "Methods for Measurement of Development Parameters in the Manufacturing Line for Use in Photolithography Modeling," *IEEE Transactions on Semiconductor Manufacturing*, Vol. 9, No. 2, May 1996, pp182-190.
8. Mack, C.A. et al., "Modeling of Solvent Evaporation Effects for Hot Plate Baking of Photoresist," *Advances in Resist Technology and Processing X*, Vol. 2195, SPIE, 1993, pp584-595.